Occult lumbar lateral spinal stenosis in neural foramina subjected to physiologic loading.

B H Nowicki, V M Haughton, T A Schmidt, T H Lim, H S An, L H Riley, 3rd, L Yu and J W Hong

AJNR Am J Neuroradiol 1996, 17 (9) 1605-1614
http://www.ajnr.org/content/17/9/1605

Occult Lumbar Lateral Spinal Stenosis in Neural Foramina Subjected to Physiologic Loading

Bruce H. Nowicki, Victor M. Haughton, Timothy A. Schmidt, Tae-Hong Lim, Howard S. An, Lee H. Riley III, Liyuan Yu, and Jung-Wha Hong

PURPOSE: To measure the effect of extension, flexion, lateral bending, and axial rotation loads applied to the spine on the anatomic relationship of the spinal nerves in the neural foramen to the ligamentum flavum and the intervertebral disk; and to determine the effect of disk degeneration on the response to loading. **METHODS:** Cadaveric lumbar motion segments were examined with CT and MR imaging, loaded with pure moment forces, frozen in situ, reexamined with CT, and sectioned with a cryomicrotome. The morphology of the intervertebral disks was classified on the basis of the appearance of the cryomicrotome sections. The neural foramina were classified as having no evident stenosis, as being stenotic, as having occult stenosis, or as showing resolved stenosis on the basis of the images and sections before and after loading. The stenotic and nonstenotic foramina were stratified by disk level, intervertebral disk classification, and type of loading applied. The effect of spinal level, disk type, and load type on the prevalence of stenosis was studied. **RESULTS:** On average, extension, flexion, lateral bending, and axial rotation resulted in the ligamentum flavum or intervertebral disk contacting or compressing the spinal nerve in 18% of the neural foramina. Extension loading produced the most cases of nerve root contact, and lateral bending produced the fewest cases. Each of the loading types resulted also in diminished contact between the spinal nerve and the intervertebral disk or ligamentum flavum in some cases. Disk degeneration significantly increased the prevalence of spinal stenosis. All foramina associated with advanced disk degeneration and half of the foramina associated with disks having radial tears of the annulus fibrosus either developed occult stenosis or were stenotic before loading. **CONCLUSIONS:** The study supports the concept of dynamic spinal stenosis; that is, intermittent stenosis of the neural foramina. Flexion, extension, lateral bending, and axial rotation significantly changed the anatomic relationships of the ligamentum flavum and intervertebral disk to the spinal nerve roots.

Index terms: Foramina, vertebral; Nerves, spinal; Spine, anatomy; Spine, stenosis

AJNR Am J Neuroradiol 17:1605–1614, October 1996

Imaging studies and myelography are used routinely to examine patients with suspected spinal stenosis. Despite the general confidence that the imaging studies are accurate, the rate of occurrence of false-negative interpretations of spinal stenosis may be as high as 30% (1). Contributing to the high false-positive rate is the 20% frequency of asymptomatic narrowing of the spinal canal and neural foramina (2). Symptomatic narrowing of the spinal canal or neural foramina is not accurately differentiated from incidental changes in the spine.

The dimensions and anatomic relationships of the neural foramina are constantly changing during normal daily activities. Therefore, spinal stenosis may be an intermittent and dynamic process in some spines. Critical narrowing of the neural foramina, inapparent on conventional computed tomographic (CT) and magnetic resonance (MR) studies, may occur when loads are applied to the spine (3). A single set of images made with the patient in the supine po-

Received January 22, 1996; accepted after revision April 23.

This work was supported in whole by NIH grant #RO1 AR33667–08.

From the Departments of Radiology (B.H.N., V.M.H., T.A.S., L.Y.) and Orthopaedic Surgery (T-H.L., H.S.A., L.H.R., J-W.H.), the Medical College of Wisconsin, Milwaukee.

Address reprint requests to Victor M. Haughton, MD, Department of Radiology, the Medical College of Wisconsin, 9200 W Wisconsin Ave, Milwaukee, WI 53226.

AJNR 17:1605–1614, Oct 1996 0195-6108/96/1709–1605

sition may not accurately represent the degree or probability of stenosis within the neural foramina or spinal canal. Therefore, the hypothesis tested was that normal physiological loads applied to the spine produce intermittent stenosis of the neural foramina. The effect of radial tears of the annulus fibrosus or advanced degeneration of the intervertebral disk on the risk of occult spinal stenosis was evaluated.

Materials and Methods

Thirty-one cadavers were selected from the Body Donation Program within 48 hours after death. Bodies with a history of metastatic disease, spine trauma, spinal surgery, or significant spinal symptoms were excluded. Lumbar spinal columns were harvested by means of blunt and sharp dissection. The surrounding paraspinal and supraspinal muscles, connective tissue, and fat were removed while the ligaments and the neural elements were preserved. Lumbar motion segments, consisting of two vertebrae and an intervertebral disk, were harvested from the spinal columns and sealed in plastic bags to prevent dehydration. Sixty-eight motion segments (136 neural foramina) were harvested from the lumbar spines of cadavers (16 male and 15 female) ranging in age from 39 to 87 years.

The motion segments were warmed to room temperature and imaged in a 1.5-T MR scanner with a 5-inch diameter send-and-receive solenoid coil. T1-weighted and T2-weighted axial and parasagittal images were obtained with a spin-echo sequence. T1-weighted axial images were obtained with parameters of 650/40/2 (repetition time/echo time/excitations), 1-mm section thickness, 8-cm^2 display field of view, and 512 × 256 matrix. Long-repetition-time axial and parasagittal images were obtained with 2000/33/2 and 2000/80/2, 1-mm section thickness, 8-cm-diameter display field of view, and 512 × 256 matrix. After MR imaging, the motion segments were stored at −20°C in plastic bags.

The superior and inferior vertebrae of the motion segment were embedded in polymethylmethacrylate (PMMA) and reinforced with 3/8-inch fiberglass rods to form 5 × 5-inch bases. Rods were inserted anteroposteriorly and transversely through each vertebral body and extended 1/2 inch out of the PMMA blocks. In the inferior PMMA cap, four 1/2-inch-diameter threaded fiberglass bolts were embedded at set locations to secure the specimen to the CT scanning platform or to the platform of the loading frame for biomechanical tests. After embedding in PMMA, the specimens were frozen at −20°C.

The frozen lumbar motion segments were imaged in a high-speed helical CT scanner. The inferior base of the specimen was bolted to a Lexan positioning plate. The positioning plate was inserted into slots on a Lexan scanning platform that straddles the CT gantry to position the specimen for imaging in the direct axial and sagittal projections. The specimen was aligned with the CT scanner's neon-helium laser lights and positioned within the isocenter of the CT gantry. Axial and parasagittal images were obtained through the entire volume of the specimen. Images were acquired with 120 kV, 200 mA, 2-second scan duration, medium body calibration, 10-cm field of view, 512 × 512 matrix, and 1-mm-thick contiguous sections.

The base of the specimen was removed from the CT scanner and bolted to a specially designed metal frame for biomechanical testing. By means of a loading arm attached to the fiberglass rods in the superior base, loads were applied to produce pure moments in flexion, extension, lateral bending, or axial rotation. The moment loads were applied in steps of 0, 0.5, 1.6, 3.6, 4.7, 5.7, and 6.6 Nm. A moment arm of 530 mm and dead weights of 100, 300, 500, 700, 900, and 1100 g were used. The loading sequences were varied systematically. After the application of the last load, the specimen was frozen in situ (under load) with liquid nitrogen and dry ice. CT was performed after loading on the frozen specimen with the techniques described.

After CT imaging, the motion segment was sectioned with a cryomicrotome in the same parasagittal plane used in the CT examinations. Photographs of the sectioned surface of the specimen were obtained at 1-mm intervals using a macrophotography system and color reversal film and compared with the corresponding MR and CT studies.

The intervertebral disks were classified on the basis of their appearance on the MR images and cryotome sections as *normal* if the disk space height, MR signal intensity, and margins of the disk were normal; as showing *aging* if the height and signal intensity were normal but concentric and transverse tears were present in the annulus fibrosus; as having a *radial tear* of the annulus fibrosus (degenerated) if a radial tear was present with or without decreased MR signal intensity, diminished disk height, or bulging of the annulus fibrosus; and as showing *advanced degeneration* if the disk height was less than half of normal (Fig 1). The motion segments were stratified by disk level, morphologic or degenerative changes in the disk, and the type of loading applied.

The neural foramina were classified according to their appearance on the MR images and cryomicrotome sections as *stenotic* if the intervertebral disk or ligamentum flavum compressed or contacted the spinal nerve in a neural foramen both before and after loading. A *compressed* nerve was defined as one whose contour was flattened or distorted by the intervertebral disk or ligamentum flavum (Fig 2). A *contacted* nerve was defined as one that retained its normal shape while in contact with the ligamentum flavum or the intervertebral disk (Fig 3). If nerve root contact or compression was identified only after the load was applied to the motion segment, the neural foramen was classified as having *occult* stenosis (Fig 4). When the contact or compression was present only before loading (but not after loading), the foramen was classified as having *resolved* stenosis (Fig 5). The number of neural foramina that had no stenosis, that were stenotic, that had occult stenosis, and that showed resolved stenosis was

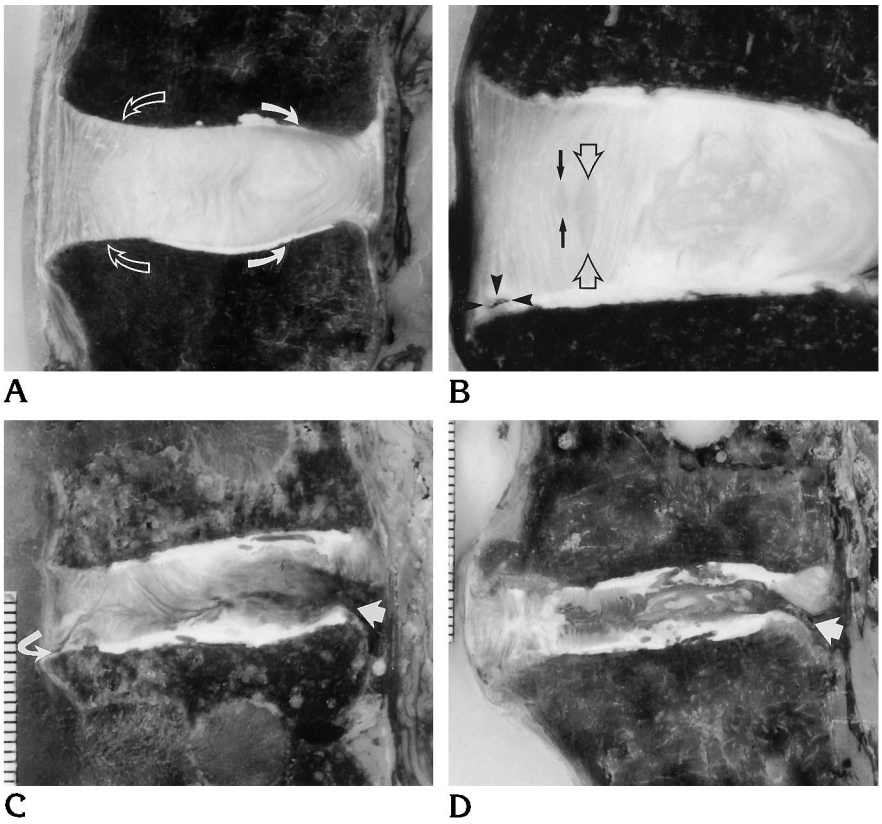

Fig 1. Parasagittal cryomicrotome sections illustrating the four different types of intervertebral disk.

A, Example of a normal (L4–5) disk. Note the distinctness of the anterior (*open arrows*) and posterior (*solid arrows*) lamellae of the annulus fibrosus.

B, Example of an aging (L1–2) disk with a prominent concentric tear (*open arrowheads*) and another smaller concentric tear (*arrows*) in the mid–anterior aspect and a transverse tear (*solid arrowheads*) in the anterior, inferior aspect of the annulus fibrosus.

C, Example of a radial tear (L3–4 disk) of the annulus fibrosus extending along the equator from the anterior (*curved arrow*) to the posterior (*straight arrow*) margins.

D, Example of an advanced degenerated (L5-S1) disk in which the lamellae of the anterior annulus fibrosus are completely disrupted and the posterior annulus is displaced superoposteriorly with a radial tear (*arrow*) in the inferior aspect. The disk height is reduced as well.

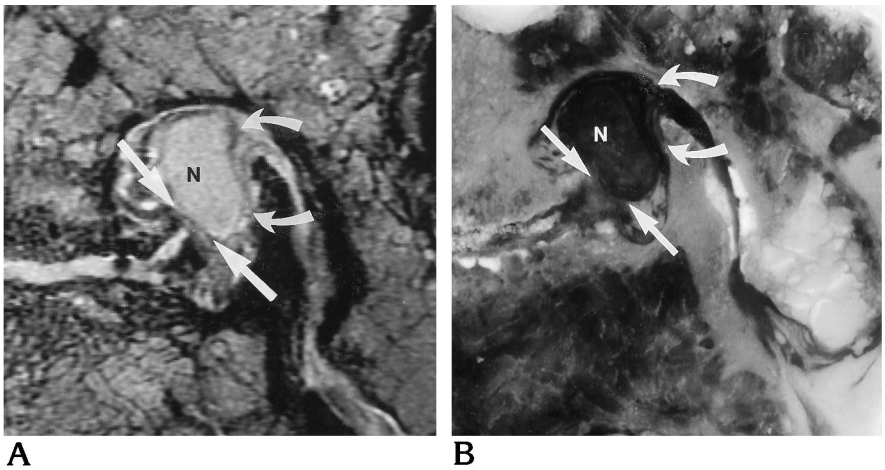

Fig 2. Illustrations of nerve root compression in the L5-S1 neural foramina.

Parasagittal preloading MR image (*A*) and corresponding postloading cryomicrotome section (*B*) of a stenotic neural foramen associated with an advanced degenerated L5-S1 disk. The nerve root (*N*) is compressed by both the intervertebral disk margin (*straight arrows*) and the ligamentum flavum (*curved arrows*). Cryomicrotome section shows the posterior aspect of the nerve root (*N*) compressed by the ligamentum flavum (*curved arrows*) and the anterior aspect of the nerve root compressed by the posterolateral margin of the intervertebral disk (*straight arrows*). Note that the anteroposterior diameter of the nerve root is reduced and its cephalocaudal diameter has increased from the compression.

tabulated and stratified by disk level, disk morphologic type, and load type. The hypothesis was tested that disk level is an important factor in the production of stenosis. The probability that stenosis was randomly distributed among levels was tested. The frequency of each type of stenosis in normal disks, aging disks, disks with radial tears, and disks with advanced degeneration was calculated. The relationship of dynamic stenosis to loading type was studied by measuring the frequency of stenosis for each type of load. The significance of the distributions was tested with one-way analysis of variance.

Results

By the anatomic criteria, six disks were classified as normal, 40 as showing aging, 15 as having radial tears (degenerated), and seven as showing advanced degeneration. The number

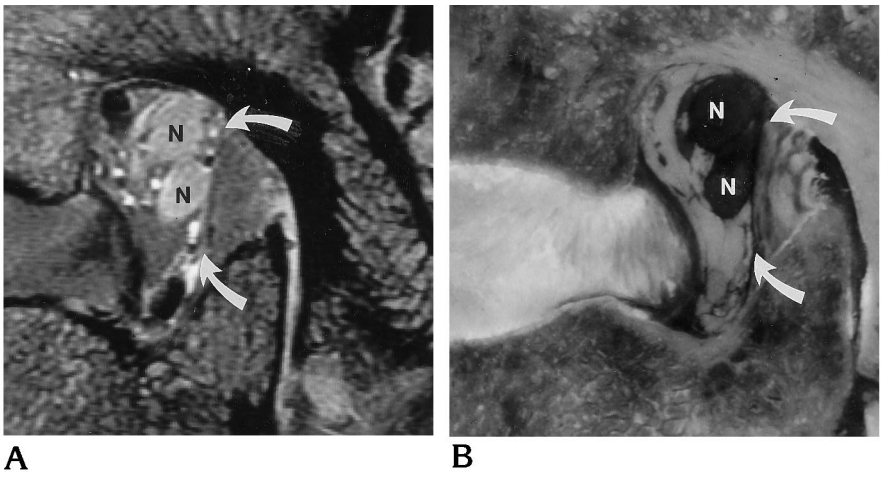

Fig 3. Parasagittal MR image (*A*) and corresponding cryomicrotome section (*B*) of a neural foramen at the L5-S1 level in which the ligamentum flavum (*arrows*) contacts but does not compress the nerve roots (*N*).

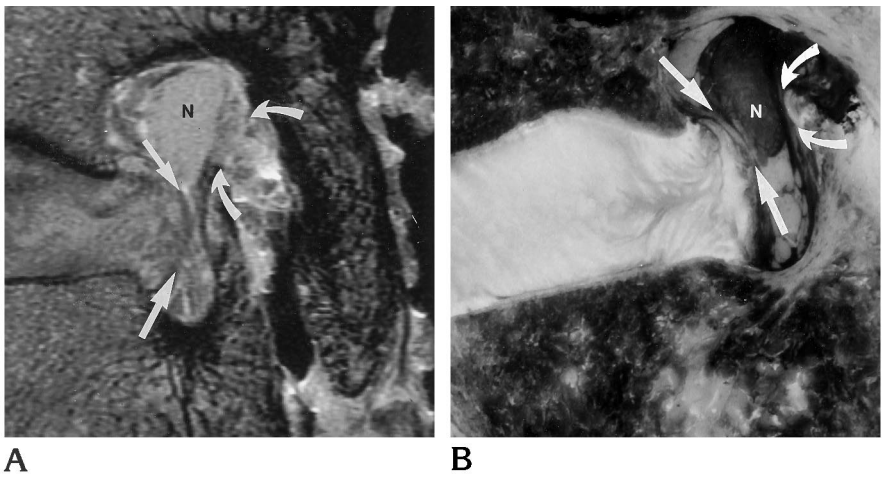

Fig 4. Illustration of occult stenosis with nerve root compression in the neural foramen at the L5-S1 level associated with a posterior radial tear in the intervertebral disk.

A, Preloading MR image shows the posterolateral intervertebral disk margin (*straight arrows*) and the ligamentum flavum (*curved arrows*) margin close to, but not contacting, the nerve root (*N*).

B, Postloading cryomicrotome section shows the posterior aspect of the nerve root (*N*) compressed by the ligamentum flavum (*curved arrows*) and the anterior aspect of the nerve root compressed by the posterolateral margin of the intervertebral disk (*straight arrows*). Note that the anteroposterior diameter of the nerve root is reduced and the cephalocaudal diameter has increased from the compression.

of specimens frozen in extension was 15; in flexion, 16; in lateral bending, 20; and in rotation, 17. The number of intervertebral disks from each disk level was: T12-L1, 15; L1–2, 12; L2–3, 11; L3–4, 12; L4–5, nine, and L5-S1, nine.

Before loading, compression of the spinal nerve was evident in five (4%) of the 136 neural foramina. Compression was due to the intervertebral disk and ligamentum flavum in two of the five specimens; the ligamentum flavum alone compressed the nerve in two cases; the nerve root was compressed by the ligamentum flavum and contacted by the intervertebral disk in one neural foramen. Contact between the spinal nerve and either the ligamentum flavum or intervertebral disk was evident in 45 additional neural foramina (33% of the 136 total studied). In these cases, the contact was due to the ligamentum flavum (36 [80%] of the cases) or to the combination of the ligamentum flavum and the disk (seven [16%] of the cases), or to the disk alone (two [4%] of the cases). A summary of the percentage of neural foramina with stenosis (that is, those cases with spinal nerve compression or contact) is presented in Table 1. The frequency of foramina that were stenotic both before and after loading was 15%; the frequency of occult stenosis (that is, contact or compression of the spinal nerve in the neural foramina only after loading) was 18%; and the frequency of resolved stenosis (that is, contact or compression before loading but not after) was 22%. Forty-five percent of the foramina were not stenotic.

In the 30 neural foramina in which the extension loading moment was applied, occult stenosis occurred in 10 (33%), which compares with

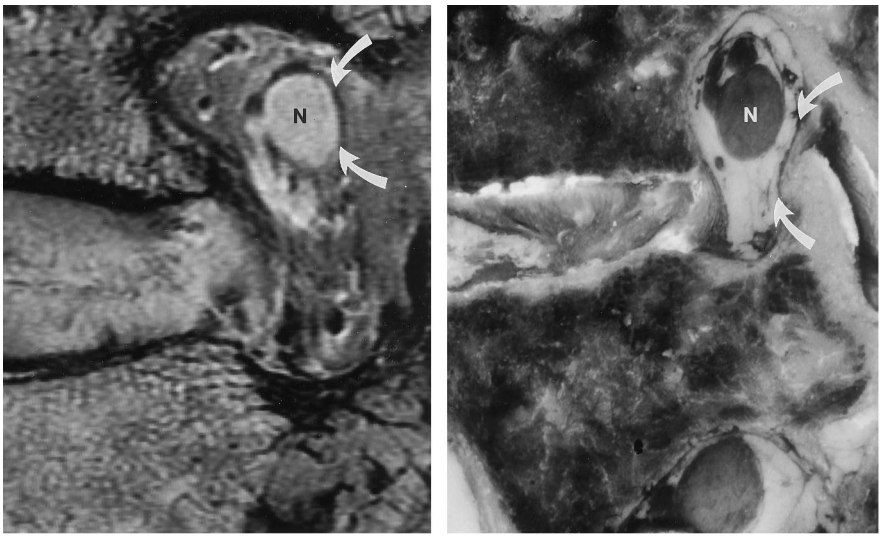

Fig 5. Example of a case of neural foraminal stenosis that resolved after loading.

A, Preloading parasagittal MR image in which the ligamentum flavum (*arrows*) margin contacts but does not compress the nerve root (*N*).

B, Postloading cryomicrotome section in which the nerve root (*N*) is separated from the ligamentum flavum (*arrows*) and the intervertebral disk margin by areolar connective tissue.

TABLE 1: Neural foramina that have no stenosis, stenosis, occult stenosis, and resolved stenosis by the type of loading applied

Load Type	n	No Stenosis, n (%)	Stenosis, n (%)	Occult Stenosis, n (%)	Resolved Stenosis, n (%)
Extension	30	17 (57)	3 (10)	10 (33)	0 (0)
Flexion	32	8 (25)	5 (16)	6 (19)	13 (41)
Lateral bending (concave sides)	20	9 (45)	3 (15)	2 (10)	6 (30)
Lateral bending (convex sides)	20	11 (55)	4 (20)	1 (5)	4 (20)
Axial rotation (leading sides)	17	7 (41)	2 (12)	3 (18)	5 (29)
Axial rotation (lagging sides)	17	9 (53)	3 (18)	3 (18)	2 (12)
Total (average)	**136**	**61 (45)**	**20 (15)**	**25 (18)**	**30 (22)**

Note.—Percentages are based on the total number of foramina of each loading type.

the 18% average for all loading types. Occult stenosis was significantly more frequent in this loading group than in the other groups ($P = .016$). Occult stenosis was due to contact by the ligamentum flavum in eight neural foramina (27%), and was due to contact with the ligamentum flavum and the intervertebral disk in one foramen (3%). In one case of occult stenosis, the nerve contact with the intervertebral disk was resolved by extension loading, but contact between the nerve and the ligamentum flavum occurred. No cases of nerve root compression resulting from extension were identified. The prevalence of resolved stenosis in the extension group was 0%, which compares with an average of 22% for all loading types.

Among the 32 neural foramina subjected to a flexion loading moment, resolved stenosis occurred in 13 (41%), which was the highest percentage of resolved stenosis for any load. Occult stenosis occurred in six cases (19%), which was near the average. Occult stenosis was due to contact between the ligamentum flavum and nerve root in four neural foramina and to contact of both the ligamentum flavum and the intervertebral disk in one foramen. In one specimen, nerve contact with the intervertebral disk was resolved by flexion loading, but contact between the nerve and the ligamentum flavum occurred. In resolving stenosis, contact between the nerve root and the ligamentum flavum or the intervertebral disk was present in 12 cases before loading; contact between the nerve root and both the intervertebral disk and the ligamentum flavum was resolved in one neural foramen by the flexion moment. One foramen

with spinal nerve compression was not relieved by the flexion moment.

For left and right lateral bending moments, the frequency of stenosis, occult stenosis, and resolved stenosis was close to average. Occult stenosis was due to contact rather than compression by the ligamentum flavum or intervertebral disk. Ten foramina were found to have contact between the nerve root and the ligamentum flavum that was relieved by the loading, but the one foramen with spinal nerve compression before loading was not relieved.

For the specimens subjected to left and right axial rotation, the frequency of stenosis, occult stenosis, and resolved stenosis was close to the averages for all groups. In four foramina with occult stenosis, contact was noted between the spinal nerve and the ligamentum flavum. In two foramina with occult stenosis, spinal nerve root compression by the intervertebral disk margin or the ligamentum flavum was observed after loading. In seven foramina with contact between the spinal nerve and the ligamentum flavum or the intervertebral disk, the stenosis was relieved by loading. In three foramina with compression of the spinal nerve before loading, the stenosis was not relieved.

A summary of the frequency by spinal level for no stenosis, stenosis, occult stenosis, and resolved stenosis in the neural foramina is presented in Table 2. Stenotic neural foramina were most frequent at the L5-S1 disk level. Occult stenotic or resolved stenotic foramina were distributed throughout the lumbar spine disk levels. The differences in the frequency of stenosis, occult stenosis, or resolved stenosis among disk levels were not significant.

The effect of the morphologic characteristics of the intervertebral disk on the frequency of foraminal stenosis is shown graphically in Figure 6. The frequency of nonstenotic foramina varied from 100% for normal disks to 0% for disks with advanced degeneration. Stenosis unchanged by loading was found in 0% of the foramina associated with normal disks, in 8% of foramina associated with aging disks, in 30% of foramina associated with radial tears, and in 50% of foramina associated with advanced degenerated disks. The relationship between disk classification and stenotic foramina was statistically significant ($P < .05$). Dynamic stenosis (that is, occult or resolving stenosis) occurred at levels with aging disks, disks with radial tears, or disks with advanced degeneration. The effect of disk classification on dynamic stenosis was not significant ($P = .831$).

TABLE 2: Neural foramina that have no stenosis, stenosis, occult stenosis, and resolved stenosis by intervertebral disk level

Disk Level	Foraminal Totals			
	No Stenosis			
	Normal	Aging	Radial Tear	Degenerated
T12-L1	2	12	1	0
L1-2	4	9	2	0
L2-3	2	6	3	0
L3-4	2	6	1	0
L4-5	0	6	1	0
L5-S1	2	2	0	0
Total	**12**	**41**	**8**	**0**
	Stenosis			
	Normal	Aging	Radial Tear	Degenerated
T12-L1	0	2	0	0
L1-2	0	0	1	2
L2-3	0	2	0	1
L3-4	0	0	2	1
L4-5	0	2	1	0
L5-S1	0	0	5	3
Total	**0**	**6**	**9**	**7**
	Occult Stenosis			
	Normal	Aging	Radial Tear	Degenerated
T12-L1	0	4	1	0
L1-2	0	0	1	0
L2-3	0	2	1	1
L3-4	0	4	1	1
L4-5	0	3	1	2
L5-S1	0	2	0	0
Total	**0**	**15**	**5**	**4**
	Resolved Stenosis			
	Normal	Aging	Radial Tear	Degenerated
T12-L1	0	8	0	0
L1-2	0	3	2	0
L2-3	0	2	2	0
L3-4	0	4	2	0
L4-5	0	1	1	0
L5-S1	0	0	1	3
Total	**0**	**18**	**8**	**3**

The relationship of occult and resolved stenosis to the type of loading and type of intervertebral disk morphology is shown in Figure 7. Occult stenosis did not occur in neural foramina associated with normal disks when extension, flexion, lateral bending, and axial rotation loading moments were applied to the motion segments. Extension produced occult stenosis in seven (44%) of the neural foramina associated

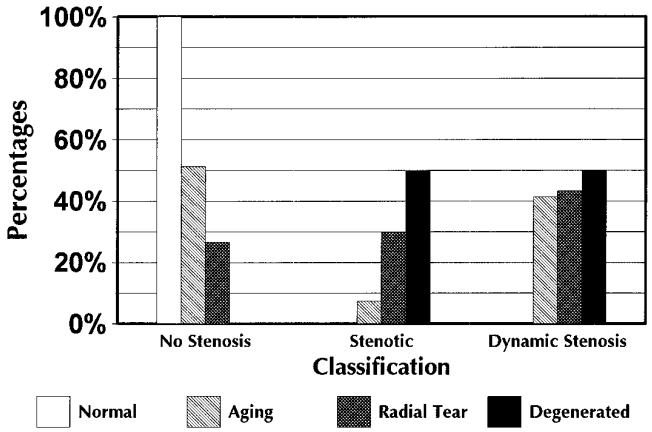

Fig 6. Graphic representation of stenosis by the type of loading and disk morphology.

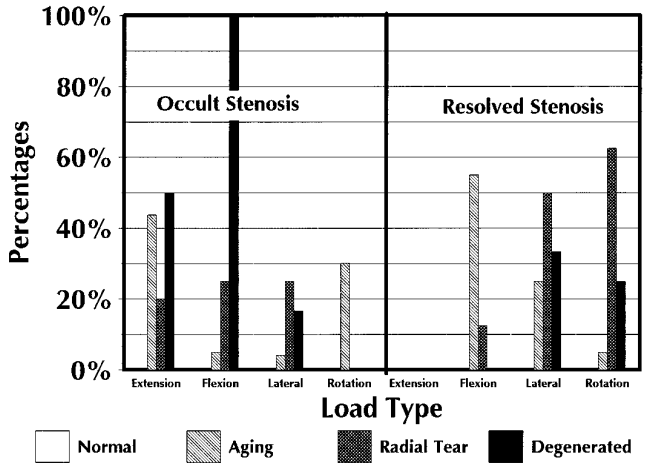

Fig 7. Graphic representation of the relationship of occult and resolved stenosis to the type of loading and disk morphology.

with aging disks, in two (20%) of the neural foramina associated with radial tears of the annulus fibrosus, and in one (50%) of the foramina associated with an advanced degenerated disk. Although flexion tended not to produce occult stenosis, occult stenosis was produced in the neural foramina when the flexion moment was applied in one (5%) of the aging disks, in two (25%) of the specimens with a radial tear of the annulus fibrosus, and in two (100%) of the neural foramina with advanced disk degeneration. Occult stenosis was evident from lateral bending in one (4%) of the neural foramina of the aging disks, in one (25%) of the neural foramina with a radial tear, and in one (17%) of the neural foramina with an advanced degenerated disk. Axial rotation produced occult stenosis in six (30%) of the neural foramina with aging disks but in none of the neural foramina associated with radial tears or advanced disk degeneration. The effect of disk classification on the frequency of occult stenosis in extension, lateral bending, and axial rotation loading was not statistically significant.

Resolved stenosis occurred with flexion, lateral bending, and axial rotation but not with extension. Flexion resolved stenosis in 55% of the aging disks and in 13% of the radial tear disks, but it did not resolve the stenosis in the degenerated disks. Lateral bending and axial rotation resulted in cases of resolved stenosis in motion segments with aging disks (25% and 5%, respectively), radial tear disks (50% and 63%, respectively), and advanced degenerated disks (33% and 25%, respectively). Differences due to disk morphology type were not significant.

The overall prevalence of neural foraminal stenosis, whether stenotic, occult, or resolved, was 100% (14 of 14) for advanced degenerated disks, 73% (22 of 30) for disks with radial tears, 49% (39 of 80) for aging disks, and 0% (0 of 12) for normal intervertebral disks.

Discussion

This study supports the concept of dynamic spinal stenosis. Positional changes and physical activity that produce flexion, extension, lateral bending, or axial rotation in the lumbar spine affect the anatomic relationship of the nerve root and adjacent connective tissues. The study shows that all four loading moments produced examples of occult stenosis; that is, contact or compression between the spinal nerve root and the ligamentum flavum or the intervertebral disk. The ligamentum flavum contacted or compressed the spinal nerve much more commonly than did the intervertebral disk. Axial rotation was the one loading moment that produced occult nerve root compression. Resolved stenosis (that is, stenosis that was relieved by the application of the moment forces) was observed but compression of a spinal nerve before loading tended not to be relieved by the application of the loads to the spine.

Our study is consistent with studies in which the dimensions of neural foramina were significantly affected by the application of force to the spine (3, 4). Extension significantly decreases the cross-sectional area of the neural foramen and its midsagittal and sagittal subarticular di-

ameters, and it causes posterior vertebral translation and disk bulging (3). Flexion increases all foraminal dimensions significantly, and decreases the thickness of the ligamentum flavum. The occurrence of occult stenosis in flexion in our study was unexpected. In neural foramina with contact between the nerve root and the ligamentum flavum or intervertebral disk, the dimensions of the foramina are smaller. With reduced disk heights and foraminal dimensions, nerve root compression is more likely (3).

The study also shows that stenosis of the neural foramina is significantly associated with disk classification. As intervertebral disk morphology progresses from normal to aging, and from radial tear to advanced degeneration, the risk of neural foraminal stenosis increases. Foraminal stenosis, either occult or present before loading, was observed in every case of advanced degeneration, in three-quarters of the radial tears, in half of the aging disks, and in none of the normal disks. Intervertebral disk degeneration did not significantly affect the risk of dynamic stenosis: the prevalence in association with aging, radial tears (degeneration), and advanced degeneration was similar, although higher than in normal disks. For some loads, disk degeneration was a factor in the prevalence of occult or resolved stenosis.

The applications of this cadaveric study to human physiology has limitations. Since the number of specimens in each loading force category is small, statistical aberrations cannot be excluded. However, the degenerative changes were evenly distributed among the different disk levels and loading categories. Our anatomic and radiologic criteria for classifying the morphologic changes in the intervertebral disk differ from those of Nachemson (5) and Galante (6), which are based on the color, appearance, distinctiveness of the nucleus pulposus or annulus fibrosus, and amount of fibrous tissue and number of fissures evident on transsected disks. Because of its biomechanical significance (7–12), a radial tear was classified with disk degeneration whereas concentric tears, transverse tears, and increasing collagen concentration were classified with aging of the intervertebral disk. In comparison with others (5, 6), our system classifies more disks as normal or as showing aging and fewer as degenerated. This study is limited by the low prevalence of normal intervertebral disks and the advanced ages of the cadavers. No stratification of the data by age was attempted because of the relative preponderance of older cadavers. The forces applied to the spinal motion segments separated from their muscle attachments cannot be extrapolated easily to in vivo loading levels. The forces applied to the motion segments were calculated to represent effects that are likely to occur with normal physiological loading of the spine. The moments applied were below levels at which vertebral bodies or intervertebral disks typically fail. The stresses received by spinal motion segments in vivo most likely equal or exceed those applied in vitro in this study. The moments applied probably produced coupled motions, since neither lateral bending nor axial rotation produced different effects on the concave and convex or the leading and lagging foramina, respectively. The specimens were not subjected to an axial load so that the effects of extension, flexion, lateral bending, and axial rotation loading moments could be studied selectively. In previous studies, axial loading has been shown to increase the diameter of the intervertebral disk and to reduce the neural foramina area, especially when there is a radial tear of the annulus fibrosus (4). The dimensions of the soft tissues and neural foramina in vitro may not precisely match those in vivo; however, the relative effect of different moments on the anatomic relationships in the neural foramina is demonstrated by this in vitro study.

The clinical significance of nerve root compression and contact in the pathogenesis of lower back pain is not addressed in this study. Since cadavers were used rather than living subjects, the question of whether the stenotic conditions observed in these studies are symptomatic cannot be answered. Contact and compression of the spinal nerve root were used as markers to compare the relative capacity of the neural foramina under different loading conditions. The capacity of the neural foramen is significantly affected by the application of force to the spine. In previous studies, the number of critically narrowed neural foramina was nearly doubled by extension and halved by flexion (3). The ligamentum flavum, much more frequently than the disk, causes the nerve root compression or contact.

The observations in this study are relevant to the diagnosis of lateral spinal stenosis by imaging. This study shows that spinal stenosis may be produced or relieved by the movements that

occur with normal physiological activities. Whatever imaging shows in the neural foramina of patients who are in a recumbent position, the anatomic relationships in the neural foramina are most likely different as the patient stands and carries out normal activities. In patients with signs and symptoms of lateral spinal stenosis, the presence of a radial tear of the annulus fibrosus or advanced degenerative changes in the intervertebral disk is indicative of an increased risk that the nerve root in the neural foramen may become intermittently compressed during motion or during load bearing. Nerve root contact when demonstrated by imaging may be relieved when the patient assumes a different position. Some moments, such as flexion, tend to relieve more stenosis than they produce, while others, such as extension, tend to produce more stenosis than they relieve. However, this study suggests that when imaging demonstrates nerve root compression, it is less likely that the stenosis will be relieved or resolved by normal activity. In all motion segments with advanced disk degeneration, nerve root contact or compression occurred at some time during the load study. On the other hand, when imaging demonstrates no nerve root effect, the nerve root may be intermittently compressed during daily activities. If CT or MR imaging show narrowing of the neural foramen without nerve root compression, that foramen may be critically narrowed so as to cause entrapment when loads are applied. The study suggests that a radial tear or advanced degeneration of the intervertebral disk increases the risk of occult stenosis because it changes the stiffness or mobility of the motion segment to specific loads or moments.

The study further suggests that the pathogenesis of radicular pain in some patients is dynamic stenosis resulting from the application of moments to the spine. Imaging the spine with the patient in a supine, non–weight-bearing position will most likely misrepresent the degree of and potential risk for spinal stenosis. Occult stenosis is more likely if the related intervertebral disk has a radial tear or advanced degeneration of the annulus fibrosus than if it has normal morphology. Previous studies suggest that radial tears of the annulus fibrosus are associated with a decrease in the stiffness or stability of motion segments and that advanced disk degeneration is associated with increased stiffness of hypomobility to specific moment loading types (13). Instability or hypermobility of the spine is theoretically a cause of lower back pain. Disk degeneration (radial tear of the annulus fibrosus) has been shown to decrease the stiffness of the intervertebral disk to axial compression (4), flexion, and axial rotation (13, 14) but not to lateral bending (13, 14). Instability of the spine is insufficiently well characterized in biomechanical terms and is inexactly diagnosed with clinical and imaging studies. This study and others suggest that certain morphologic and degenerative changes in the annulus fibrosus of the intervertebral disk affect the frequency of neural foraminal stenosis and the biomechanical stiffness of the motion segment. Strategies to image the spine under loading conditions or to determine criteria for identifying patients at risk for occult stenosis during loading of the spine may improve the clinical diagnosis of radicular pain.

Acknowledgments

We gratefully acknowledge the contributions of Cathy Biskup for providing the CT images, Lloyd Estkowski and David Horzewski for providing the MR images, David Vollmers for providing the cryomicrotome sections and photographs, and Jane Harmeyer for preparing the manuscript.

References

1. Kent DL, Haynor DR, Larson EB, Deyo RA. Diagnosis of lumbar spinal stenosis in adults: a metaanalysis of the accuracy of CT, MR, and myelography. *AJR Am J Roentgenol* 1992;158:1135–1144
2. Boden SD, Davis DO, Dina TS, Patronas NJ, Wiesel SW. Abnormal magnetic-resonance scans of the lumbar spine in asymptomatic subjects: a prospective investigation. *J Bone Joint Surg [Am]* 1990;72:403–408
3. Hasegawa T, An HS, Haughton VM, Nowicki BH. Lumbar foraminal stenosis: critical heights of the intervertebral discs and foramina. *J Bone Joint Surg [Am]* 1995;77:32–38
4. Nowicki BH, Yu S, Reinartz J, Pintar F, Yoganandan N, Haughton VM. Effect of axial loading on neural foramina and nerve roots in the lumbar spine. *Radiology* 1990;176:433
5. Nachemson A. Lumbar intradiscal pressure: experimental studies on post-mortem material. *Acta Orthop Scand Suppl* 1960;43:7–104
6. Galante JO. Tensile properties of human annulus fibrosus. *Acta Orthop Scand Suppl* 1967;100
7. Yu S, Sether LA, Ho PSP, Wagner M, Haughton VM. Tears of the annulus fibrosus: correlation between MR and pathologic findings in cadavers. *AJNR Am J Neuroradiol* 1988;9:367–370
8. Yu S, Haughton VM, Ho PSP, Sether LA, Wagner M, Ho KC. The progressive and regressive changes of the nucleus pulposus, II: the adult. *Radiology* 1988;169:93–97

9. Wagner M, Sether LA, Yu S, Ho PSP, Haughton VM. Age changes in the lumbar intervertebral disc studied with magnetic resonance and cryomicrotomy. *Clin Anat* 1988;1:93–103
10. Sether LA, Yu S, Haughton VM, Fischer ME. Intervertebral disk: normal age-related changes in MR signal intensity. *Radiology* 1990;177:385–388
11. Yu S, Haughton VM, Sether LA, Ho KC, Wagner M. Criteria for classifying normal and degenerated lumbar intervertebral disks. *Radiology* 1989;170:523–526
12. Yu S, Haughton VM, Sether LA, Wagner M. The annulus fibrosus in bulging intervertebral disks. *Radiology* 1988;169:761–763
13. Lim TH, Haughton VM, Hong JH, Nowicki B, Yu L, Yoshida H. Biomechanical characteristics of radial tear of the annulus fibrosus. *Orthop Res Soc Proc* 1996;142:24
14. An HS, Haughton VM, Lim TH, et al. The relationship between disc degeneration and kinematic characteristics of the lumbar motion segment. *Orthop Res Soc Proc* 1996;142:663

Please see the Commentary on page 1615 in this issue.